

# Characterisation of space-time variability in stratified and mixed coastal waters (Baie des Chaleurs, Québec, Canada): application of fractal theory

Laurent Seuront\*, Yvan Lagadeuc

Université des Sciences et Technologies de Lille, URA CNRS 1363, Station Marine, BP 80, F-62930 Wimereux, France

**ABSTRACT:** The variability of *in vivo* fluorescence, temperature and salinity in the vertically stratified and well-mixed waters of the Baie des Chaleurs (Québec, Canada) was investigated as a continuous function of scale by applying the concept of fractal dimension to variogram analysis. Widely applied to the description of spatial heterogeneity, fractal dimension appears here to be a helpful descriptive tool in discriminating between homogeneity and heterogeneity in time series of both physical and biological parameters. In stratified waters, the structuration of *in vivo* fluorescence, temperature and salinity remains the same over time, in spite of mixing induced by the rise of a strong wind, and is shown to be associated with the global structure of the water column. In mixed waters, the situation is more complex, giving rise to specific behaviour of *in vivo* fluorescence and salinity. In both cases, the differences observed between the fractal dimensions can be explained in terms of different ranges of scales perceived in pattern variability and thus, in the complexity of the pattern structure. We also suggest that the departure from strict selfsimilarity which seems to be associated with the vertical structure of the residual circulation is an indicator of the transitional zone between different levels of system organisation.

**KEY WORDS:** Space-time variability · Homogeneity · Heterogeneity · Fractal dimension · Stratified and mixed waters

## INTRODUCTION

Most processes in natural environments—physical forcings, population and community dynamics—are sources of heterogeneity and create space-time structures such as gradients, patches, trends or other complex patterns (Legendre & Fortin 1989, Dutilleul & Legendre 1993). These heterogeneous structures are particularly well developed in marine environments (Steele 1974, 1978, Haury et al. 1978) where resources such as plankton exhibit patchiness over a continuum of scales (Platt 1972, Mackas & Boyd 1979, Mackas et al. 1985). The multiscale variability of marine environments, outlined by Steele (1985, 1989), leads to a view of the ocean as a 'landscape' in the sense that it can be described by patterns of different temporal and spatial scales. Many physical and biological oceanographers have thus related their findings to the spectrum of physical processes, ranging from circulation patterns in

oceanic basins to large gyres, to fine-scale eddies or rips (e.g. Denman & Powell 1984, Legendre & Demers 1984, Mackas et al. 1985, Platt & Sathyendranath 1988). Ecologists have also recognised spatial heterogeneity as a major factor regulating the distribution of species (Wiens 1976, Risser et al. 1984, Urban et al. 1987). Thus, as reviewed by Wiens (1989), ecology must deal with scale, because the objects it focuses on, the organisms and types of environment, are rarely found to be homogeneously distributed through time or space. Yet until recently no quantitative nor qualitative theory has described the origin, dynamics, and consequences of heterogeneity in ways that could increase the accuracy of predictions about ecological processes in complex environments. Dealing with scales has thus been required in order to overcome the difficulties generated by space-time dependencies associated with an heterogeneous distribution of ecological variables.

Mandelbrot (1983), who recognised the ubiquity of sets that violate basic assumptions of uniformity, introduced the concept of the fractal, a geometric form

\*E-mail: seuront@loalitt.univ-littoral.fr

which exhibits structure at all scales. In heterogeneous sets, where estimates of quantities such as biomass vary precisely with the scale at which measurements are made (Burrough 1981, 1983a, Milne 1988), fractal dimension then appears to be a useful measure of space-time complexity (Phillips 1985), and provides several advantages over other descriptive indices of ecological patchiness. Classical statistical theory works well in predicting change in variance due to different sizes of sampling units or different grains of sampling strategy when the sampling units are independent. The basic assumption of independence of replicates, however, is rarely verified in natural science and, therefore, the use of classical theory is questionable. Moreover, the more traditional, widely used mathematical descriptors, such as the variance-to-mean ratio (Taylor 1961, Frontier 1972, Downing et al. 1987), have little meaning in a multiscale spatial context (Palmer 1988, Hurlbert 1990). Furthermore, space-time dependence frequently prohibits rigorous statistical analyses of ecological data, while inferences based on autocorrelated observations are risky (Bivand 1980).

The primary goal of fractal analysis and similar techniques (i.e. spectral analysis) is to describe variability over a continuum of scales. Fractal geometry is thus becoming increasingly popular among scientists and has been successfully applied to a great variety of problems involving complex patterns in nature, including terrestrial (Burrough 1981, 1983a, Krummel et al. 1987) and Martian (Woronow 1981) landscapes, cloud shapes (Lovejoy 1982), rainfall time series (Olsson et al. 1992), breaking waves (Longuet-Higgins 1994), shoreline erosion rate (Phillips 1985), and distributions of nesting bald eagles in rugged landscapes (Penny-cuick & Kline 1986). In ecology, insightful descriptions of various possible applications of fractals are given by Frontier (1987) and Sugihara & May (1990). Fractals have been used to describe habitat complexity (Bradbury & Reichelt 1983, Bradbury et al. 1984, Gee & Warwick 1994a, b), species diversity (Frontier 1985, 1994), movements of marine (Bundy et al. 1993, Erlandson & Kostylev 1995) and terrestrial (Wiens et al. 1995) invertebrates, shapes of marine snow (Li & Logan 1995, Logan & Kilps 1995) and growth processes (Kaandorp 1991, Kandoorp & Dekluijver 1992).

Basically, in ecology, 'variability' indicates changes in the values of a given quantitative or qualitative descriptor; it is distinct from 'heterogeneity' which refers to patterns and processes composed of parts of different kinds (Kolasa & Rollo 1991). This distinction is, however, not as sharp as may appear at first glance, and meanings essentially depend on the choice of approach (Downing 1991, Naeem & Colwell 1991, Shashak & Brand 1991). From a statistical viewpoint, however, 'heterogeneity', when applied to the distribution of the

values taken by a random variable, is the opposite of 'homogeneity', which refers to sameness and similarity. The degree of similarity implied by the term 'homogeneity' may vary from a minimum of a single common attribute, as in the equality of means, to the extreme of total sameness, that is, equivalence of distributions, and thus refers—in the framework of time series analysis—to a pattern of variability characterised by the closeness of scales of variations. In this paper, 'homogeneity' and 'heterogeneity' are specifically associated with patterns remaining similar upon subdivision in time—at each scale, the pattern differs but always shows the same relative variability—as strictly defined in the framework of fractal theory (Mandelbrot 1977, 1983). In that way, fractal dimensions ( $D_F$ ) appear to be helpful measures in discriminating between homogeneity and heterogeneity of space-time patterns. They reflect the balance of short-range and long-range variations and thus characterise homogeneous and heterogeneous patterns, respectively (Burrough 1981, He et al. 1994). A low  $D_F$  value means that the heterogeneity of the variable is high and there are dominant long-range effects. A high  $D_F$  characterises very complex processes where short-range, local variability is highly developed and tends to obfuscate long-range trends; the variable is thus more evenly distributed (i.e. less structured) in space and time. As an example,  $D_F \approx 2$  in a bi-dimensional space characterises regular—or homogeneous—patterns, indicating that the variation within a sampling unit will be equal to the variation among sampling units, while  $D_F < 2$  characterises more irregular—or heterogeneous—patterns.

In this paper, the concept of fractal dimensions is used in conjunction with variogram analysis, a geostatistical technique which is conceptually similar to the traditional block-size techniques of Pattern Analysis (Greig-Smith 1979), but offers the advantage of describing variation as a continuous function of scale (Palmer 1988). Fractal dimension  $D_F$  is thus regarded as an index of the complexity perceived in series of temperature, salinity and *in vivo* fluorescence recorded both in stratified and mixed waters in the Baie des Chaleurs (Québec, Canada).

## MATERIAL AND METHODS

**Sampling procedure.** Sampling was conducted in the Baie des Chaleurs from 10 to 12 September 1991 at a stratified station (20 m depth) close to Caplan, located well inside the bay, and from 20 to 22 September at a vertically mixed water column (20 m depth) at Grande-Rivière, close to the entrance of the bay (Fig. 1). At each anchor station, measurements of physical parameters (temperature and salinity) and *in vivo* fluo-

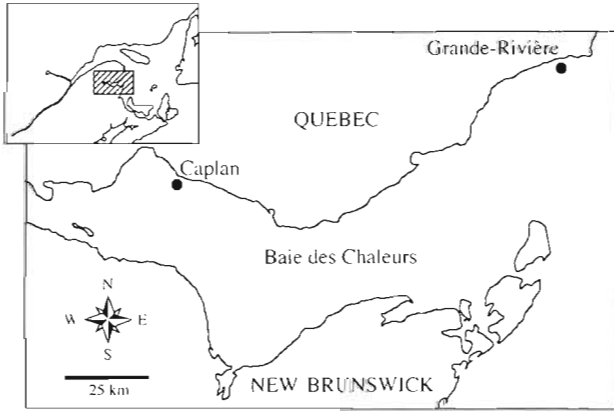


Fig. 1. Locations of the 2 anchor stations along the north shore of Baie des Chaleurs, eastern Canada

rescence (an index of phytoplankton biomass) were taken every hour from the surface to 20 m depth with a SBE 25 Sealogger CTD and a Sea Tech fluorometer over periods of 57 h at Caplan and 52 h at Grande-Rivière. Every 2.25 h, current speeds and directions were measured for 5 min at 2.5, 5, 7.5, 10, 12.5, 15, 17.5 and 20 m with an Aanderaa current meter, which was moored at 5 m during the times between profiles.

**Data analysis.** The vertical stratification of the water masses was calculated using the potential energy  $E_p$  ( $J m^{-3}$ ), which corresponds to the amount of energy required to redistribute mass in a complete vertical mixing (Simpson et al. 1979, Pond & Pickard 1983):

$$E_p = \frac{1}{H} \int_{-H}^0 (\rho - \bar{\rho}) g z \cdot dz \quad (1)$$

where  $H$ ,  $\rho$ ,  $\bar{\rho} = \frac{1}{H} \int_{-H}^0 \rho z \cdot dz$ ,  $g$  and  $z$  are the height of the water column, the density, the mean density of the water column, the gravitational acceleration ( $m s^{-2}$ ) and the depth, respectively.

The Richardson number,  $Ri$ , was used to estimate the dynamic stability of the water column (Vandevelde et al. 1987):

$$Ri = \frac{g}{\bar{\rho}} \frac{d\rho/dz}{(du/dz)^2} \quad (2)$$

where  $\rho$ ,  $g$ ,  $u$  and  $z$  are the density, the gravitational acceleration, the horizontal component of the current velocity ( $m s^{-1}$ ), and the depth, respectively. This number compares the stabilising effect of buoyancy forces (represented by the square of the Brunt-Väisälä frequency,  $d\rho/dz$ ) to the destabilising influence of vertical shear in the horizontal velocity field (represented by the square of the velocity gradient,  $du/dz$ ) over a given depth interval. Values under 0.25 indicate a potential instability, and larger values indicate a greater potential stability (Mann & Lazier 1991).

Missing data due to an inadequate ( $>1 m s^{-1}$ ) descending speed of the CTD probe were estimated using the method proposed by Zagoruiko & Yolkina (1982), which is particularly adapted to the prediction of missing data in bi-dimensional data tables. Unlike 1-dimensional interpolation techniques, such as kriging, this method provides for each missing data value a predicted value which is not limited to an intermediate value of its surrounding data in a given series but takes into account the whole data table.

To detect dates, intensity and duration of any changes in the values of a given parameter, we used the cumulative sums method (Ibanez et al. 1993). The calculation consists of subtracting a reference value (here the mean of the series) from the data; then these residuals are successively added, forming a cumulative function. Successive negative residuals produce a decreasing slope, whereas successive positive residuals create an increasing slope (the value of the slope is proportional to the mean deviation). Values not very different from the mean show no slope.

**Fractal analysis.** The concept of fractals has been recently introduced to the description of natural systems (Mandelbrot 1983) and strictly refers to geometrical patterns in which the Hausdorff-Besicovitch dimension exceeds the topological (i.e. Euclidean) dimension. In less technical terms, fractals are temporal or spatial phenomena presenting a detailed structuration at all scales, i.e. they do not lose details upon repeated magnifications or reductions. We used a method (Burrough 1981, 1983a) based on geostatistics and regionalised variable (RV) theory (Matheron 1971, Journel & Huijbregts 1978) to calculate fractal dimensions of physical parameters and *in vivo* fluorescence for each of the profiles. RVs are continuous variables whose variations are too complex to be described by traditional mathematical functions (Phillips 1985). Patterns of variation in RVs can then be expressed by their semivariance  $\gamma(h)$ , defined as:

$$\gamma(h) = \frac{1}{2N(h)} \sum_{i=1}^{N(h)} [Z(i) - Z(i+h)]^2 \quad (3)$$

where  $Z(i+h)$  is the value of the dependent variable  $Z(i)$  at a point separated from point  $i$  by distance, or lag,  $h$ , and  $N(h)$  is the number of pairs of data points separated by the lag  $h$ . The semivariogram is the plot of  $\gamma(h)$  as a function of  $h$ . The semivariance has, under certain conditions (e.g. see Berry & Lewis 1980 for further developments on the variance properties of the Weierstrass-Mandelbrot fractal function), the form of a fractal function that scales with  $h^{4-2D}$  at the origin; the fractal dimension  $D$  of the RV  $Z(i)$  can thus be estimated from the slope  $m$  of a log-log plot of the semivariogram of  $Z(i)$  (Burrough 1981, 1983a):

$$D = (4 - m)/2 \quad (4)$$

Because semivariogram estimates tend to deteriorate with increasing lag  $h$  for finite-length sample series (i.e. greater distances are more affected by low sample sizes and spurious properties of the data; Journel & Huijbregts 1978), an objective criterion is needed for deciding upon an appropriate range of  $h$  to include in the regressions. We used the values of  $h$  which maximised the coefficient of determination ( $r^2$ ) and minimised the total sum of the squared residuals for the regression.

Semivariogram analysis requires the assumption of at least reduced stationarity, i.e. the mean and the variance of a time series depend only on its length and not on the absolute time (Platt & Denman 1975, Legendre & Legendre 1984). Stationarity was tested by calculating Kendall's coefficient of rank correlation,  $\tau$ , between the series and the  $x$ -axis values in order to detect the presence of a linear trend (Kendall & Stuart 1966) [Kendall's coefficient of correlation was used in

preference to Spearman's coefficient of correlation  $\rho$ , although the latter was recommended in Kendall (1976), because Spearman's  $\rho$  gives greater weight to pairs of ranks that are further apart, while Kendall's  $\tau$  weights each disagreement in rank equally; see Sokal & Rohlf (1995) for further developments]. We thus eventually detrended the time series by fitting regressions to the original data by least squares and used the regression residuals in further analysis.

## RESULTS

### Physical data

The structure of the current speed and direction at 5 m (where the greatest number of data values were collected) presented 2 distinct patterns associated with an increase of the wind speed at Caplan and with the rise of a heavy swell at Grande-Rivière.

At Caplan, the time series could be divided in 2 parts according to the wind speed, which ranged from  $1.9 \text{ m s}^{-1}$  during the first 27 profiles to  $6.6 \text{ m s}^{-1}$  on and after the 28th profile (Lagadeuc et al. 1997). For all the profiles, current speed and direction were tidally dependent (Lagadeuc et al. 1997). However, as current direction was always directed to the west-northwest during flood and to the east-southeast during ebb, current speed depended on wind. During the first 27 profiles, current speed was less than  $5 \text{ cm s}^{-1}$  during flood, and approximately  $40$  to  $50 \text{ cm s}^{-1}$  during ebb. During windy profiles, highest speeds were observed during flood (around  $15 \text{ cm s}^{-1}$ ), while during ebb, current speeds were approximately half this value (Lagadeuc et al. 1997).

At Grande-Rivière, current speed and direction were not significantly tidally dependent (autocorrelation,  $p < 0.05$ ). However, before the swell (i.e. the first 29 profiles) the current was consistently directed to the north-northeast with a speed around  $6$  to  $8 \text{ cm s}^{-1}$ , whereas during the swell (on and after the 30th profile), the speeds were slightly higher (around  $15 \text{ cm s}^{-1}$ ) with a west-southwest direction.

The vertical structure of the water column also presented 2 distinct patterns. At Caplan, these 2 patterns are

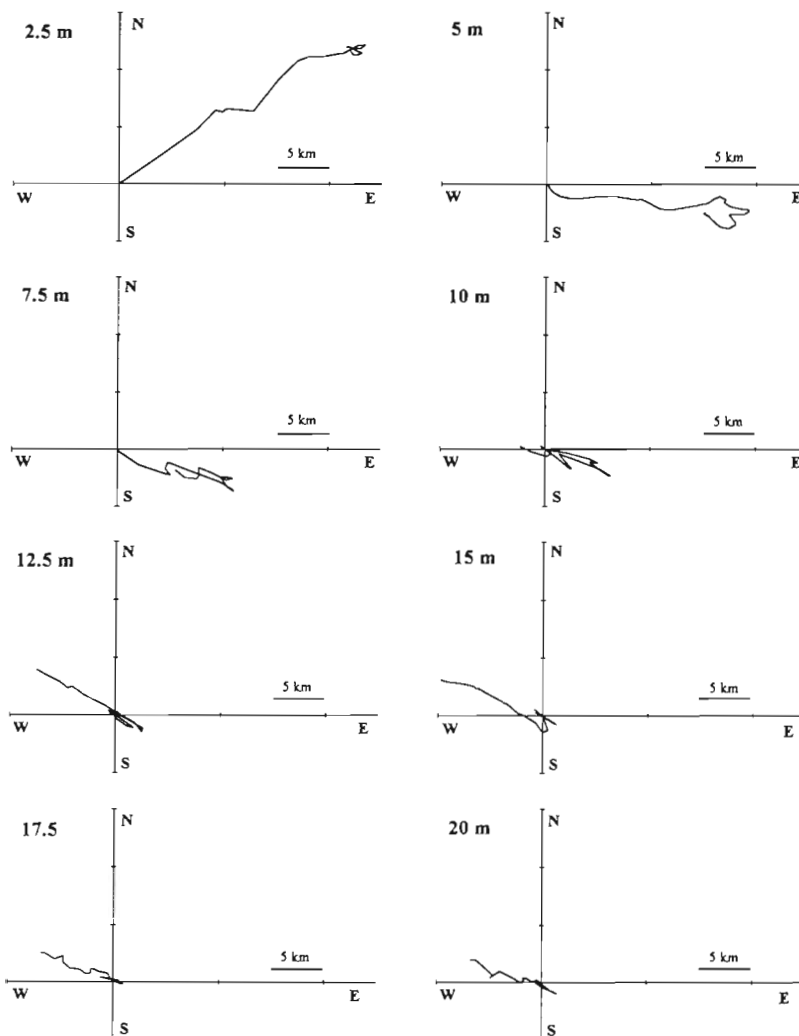


Fig. 2. Eulerian residual current in relation to depth at Caplan

perceptible from an unidirectional drift to the northeast which is stopped by the action of wind at 2.5 m (Fig. 2). For the other depths, a general pattern was observed for the effect of tide and wind on eulerian residual currents: south-eastward drift followed by north-westward drift. Moreover, the magnitude of drift decreased near bottom, where the north-westward drift due to wind was stronger than the south-eastward drift due to tide (Fig. 2). At Grande-Rivière, except at 2.5 m where the drift associated with the swell was west-north-west (Fig. 3), eulerian residual currents displayed similar patterns of variation whatever the depth: the north-north-east drift associated with tide before the swell was west-southwest thereafter (Fig. 3). As previously observed at Caplan, the amplitude of drifts decreased with depth, and the drift associated with the swell was always higher than the tidal drift (Fig. 3). In all cases, the drifts observed at Grande-Rivière were always 2 or 3 times smaller than those observed at Caplan.

During the first part of the cruise, alternative variations in intensity of stratification were tidally dependent at Caplan (Fig. 4a). Thereafter, progressive homogenisation was observed with the decrease of  $E_p$ . Dynamic stability  $Ri$  showed values less than 0.25 at the surface and near the bottom during windy profiles (Fig. 5a), which suggest a dynamic destabilisation (i.e. mixing) of the water column as opposed to the advection of mixed water. In contrast, at Grande-Rivière the water column was always homogeneous (i.e. mixed) with very low values of  $E_p$  (Fig. 4b) and values of dynamic stability  $Ri$  less than 0.25 at the surface during the 52 profiles and near the bottom, especially for profiles during swells (Fig. 5b).

### *In vivo* fluorescence

*In vivo* fluorescence exhibited a vertical gradient at Caplan during the first part of the time series in relation to the stratification of the water column (Raby et al. 1994). During the second part of the time series, the vertical gradient was destroyed by water column mixing, and phytoplankton were evenly distributed. A fluorescence maximum was observed during the first part

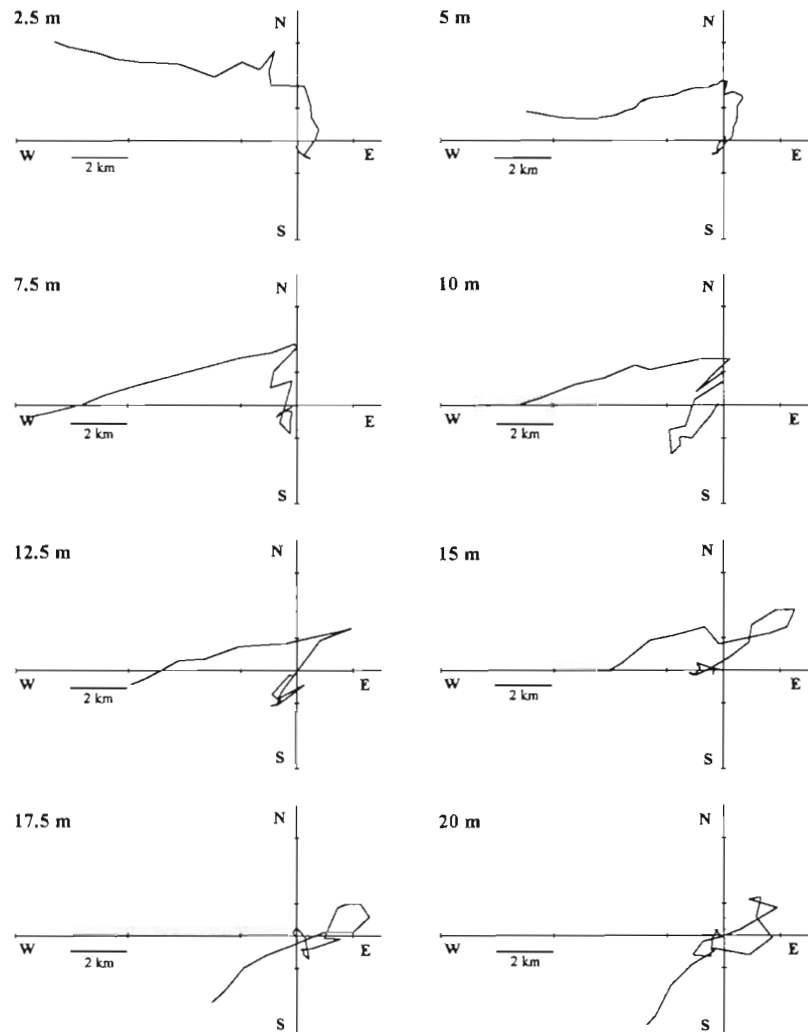


Fig. 3. Eulerian residual current in relation to depth at Grande-Rivière

of the time series in the surface layer over the thermocline and was more than twice as large as the maximum observed at Grande-Rivière, where *in vivo* fluorescence was always homogeneously distributed.

Moreover, the computation of the cumulative sum series in both cases pointed out 2 distinct patterns of variability. At Caplan, except after profile 31 when the water column was homogenised by wind, we found the following recurrent trend: an increasing slope during flood which characterised a group of values lower than the mean, followed by a decreasing slope during ebb (Fig. 6a) that characterises some values higher compared to the whole series. Chlorophyll *a* (chl *a*) and *in vivo* fluorescence being highly correlated, as shown by Raby et al. (1994) on the same set of samples, *in vivo* fluorescence fluctuations can be related to the fluctuations of phytoplankton biomass.

In contrast, at Grande-Rivière, where hydrodynamic conditions were weaker, we found a diel periodicity,

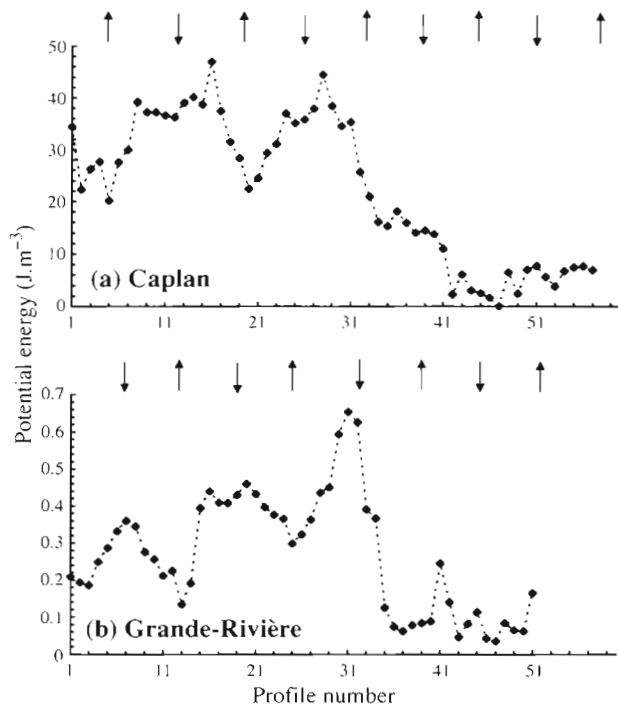


Fig. 4. Potential energy during the time series at (a) Caplan and (b) Grande-Rivière. ↑ and ↓ indicate high tide and low tide, respectively

shown by an increasing slope during nighttime (i.e. from 2 h before sunset to 2 h before sunrise) and a decreasing slope during daytime (Fig. 6b). That behaviour might correspond to the decrease of *in vivo* fluorescence around the solar midday, corresponding to photoinhibition (Falkowski & Kiefer 1985), linked to a decrease of primary production as observed by Lizon et al. (1995) in low turbulent conditions and supported by the weak correlation between fluorescence and chl *a* (Raby et al. 1994).

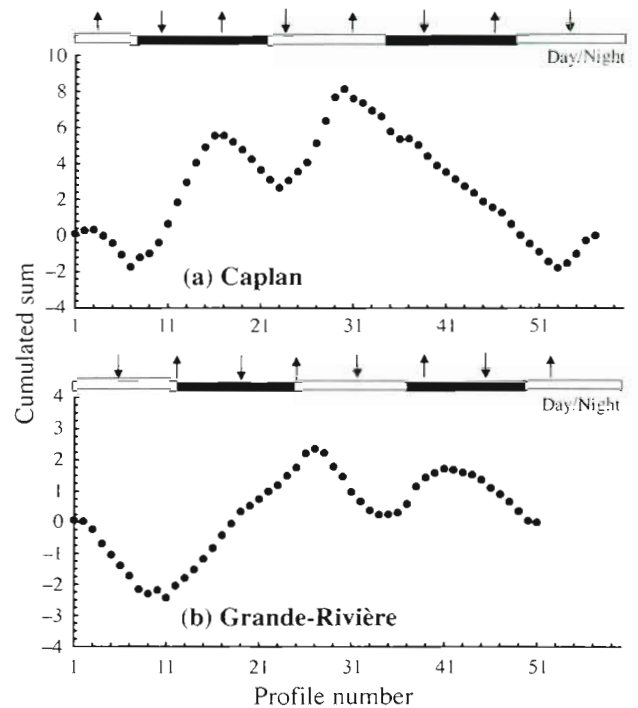
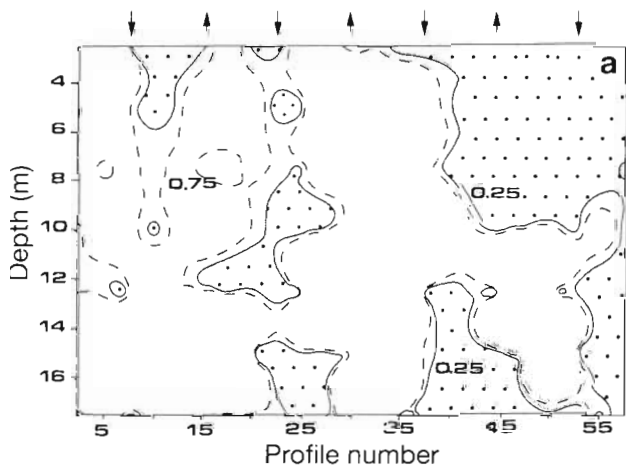


Fig. 6. Cumulative sum series of *in vivo* fluorescence at 4 m depth for (a) Caplan and (b) Grande-Rivière anchor stations. ↑ and ↓ indicate high tide and low tide, respectively

### Semivariogram analysis and fractal dimensions

The double logarithmic semivariograms for temperature, salinity and *in vivo* fluorescence time series at Caplan and Grande-Rivière together with their best fitting lines are given in Figs. 7 & 8, respectively. Only scales less than half of the total length of the data set are shown, because greater distances are more affected by low sample sizes and spurious properties of the data (Journel & Huijbregts 1978).

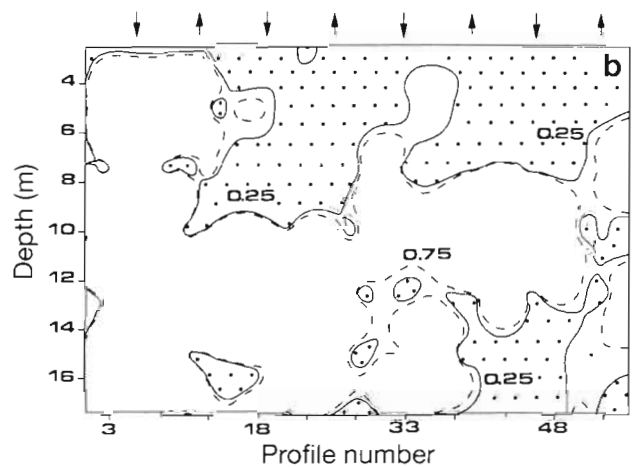


Fig. 5. Richardson number (*Ri*) in relation to depth and time at (a) Caplan and (b) Grande-Rivière. Hatched iso-*Ri* basins correspond to *Ri* < 0.25. ↑ and ↓ indicate high tide and low tide, respectively

At Caplan, temperature, salinity and *in vivo* fluorescence semivariograms exhibit similar behaviours. In the sub-surface (2 m; Fig. 7), their linearity over the whole range of time scales illustrates temporal dependence, suggesting that the same process can be regarded as the source of physical and biological patterns. This process can then be associated with the general drift to the northeast which clearly dominates the eulerian residual circulation pattern (cf. Fig. 2). From 5 to 11 m (Fig. 7); semivariograms exhibit a linear behaviour as the temporal lag increases up to 8 h. This behaviour is restricted to maximum time scales of 5 h for deeper layers. The scales of temporal dependence (i.e. semivariograms' linearity) can then be associated with characteristic time scales which are clearly depth-dependent (Fig. 7), and can be related to the progressive change in direction and intensity of the eulerian residual circulation (Fig. 2). The semivariograms are not influenced by that change of vertical structure, in spite of the transition observed between stratification and dynamic homogenisation of the water column due to the northwestward drift induced by the wind.

Indeed, semivariogram analyses conducted separately on the stratified and the mixed part of the series revealed very similar linear behaviours (Fig. 9) which are indistinguishable from each other (*t*-test,  $p > 0.05$ ; Zar 1984) and from the linear behaviour observed from the semivariogram analysis conducted on the whole series (covariance analysis, *F*-test,  $p > 0.05$ ). These results thus suggest an extreme similarity—at a given depth—between the effects of different physical forcings such as wind or tide on the temporal structuration of variability of physical and biological parameters.

At Grande-Rivière, the situation is quite different (Fig. 8). Temperature semivariograms are clearly linear over the whole range of scales from the sub-surface to 15 m depth. At deeper layers the linearity is only observed for time scales increasing up to 5–6 h. Semivariograms of salinity are linear from the sub-surface to 15 m depth as the temporal lag increases up to about 16–18 h and linear deeper for time scales of about 6–8 h. As previously suggested at Caplan, the loss of scale dependence of semivariograms seems to be associated with the vertical structuration of the residual circulation in direction and intensity (Fig. 3).

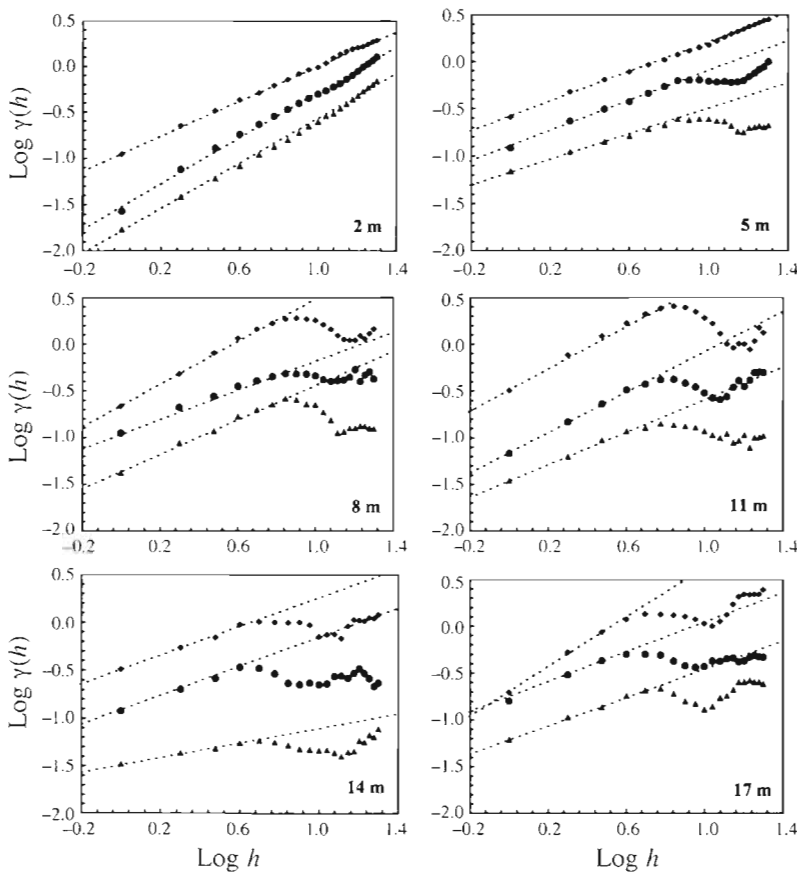


Fig. 7. Double logarithmic semivariograms of *in vivo* fluorescence ( $\blacklozenge$ ), temperature ( $\bullet$ ) and salinity ( $\blacktriangle$ ) for Caplan anchor station (curves have been vertically offset so as not to overlap). Straight dashed lines show the scaling range

On the other hand, the differences observed in the time scales at which semivariograms of temperature and salinity lose linearity could be related to the specificity of salinity which, unlike temperature, is influenced by river discharge and mixing with water masses coming from outside the bay (Le Quéré 1992, Bonardelli et al. 1993) and exhibits a general temporal evolution more irregular than temperature, essentially deeper than 15 m (Le Quéré 1992). Semivariograms of *in vivo* fluorescence were linear for time scales of 6–8 h from the sub-surface to 17 m depth, and this specific behaviour of the fluorescence semivariograms can be related to the biological activity which is quite dominant (i.e. diel periodicity; cf. Fig. 6a), in comparison with the variability observed at Caplan which is mainly dominated by physical processes (i.e. tidal periodicity; cf. Fig. 6b).

In both cases, log-log linearity of scale-invariant parts of semivariograms is very strong, with coefficient of determination ( $r^2$ ) ranging between 0.948 and 0.998 for temperature, 0.855 and 0.999 for salinity, and 0.905 and 0.999 for *in vivo* fluorescence at Caplan and 0.749 and 0.997 for temperature, 0.855 and 0.997 for salinity, and 0.959 and 0.999

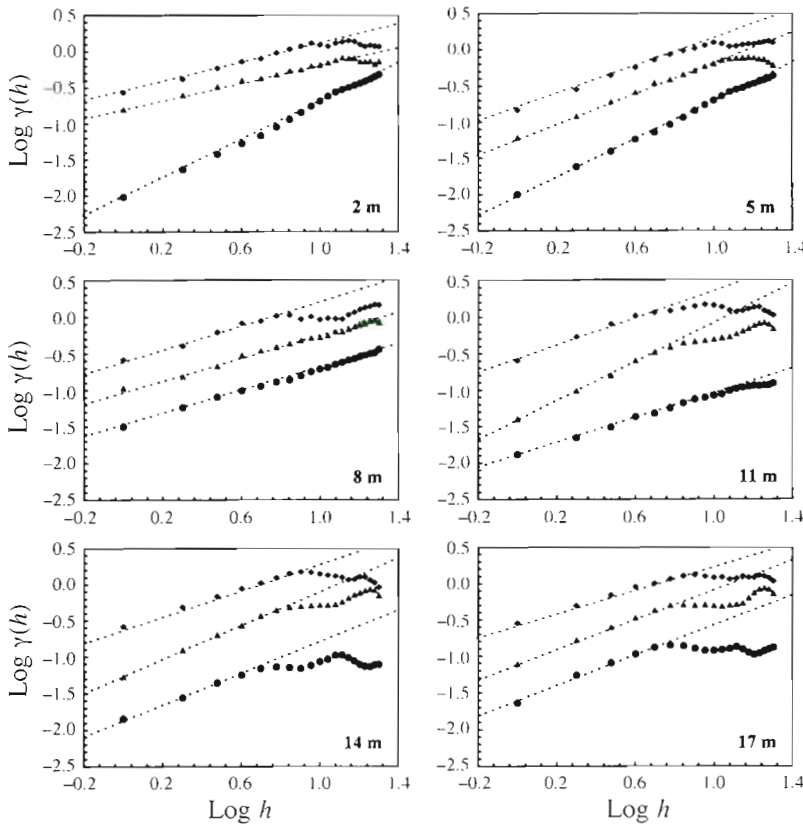


Fig. 8. Double logarithmic semivariograms of *in vivo* fluorescence (◆), temperature (●) and salinity (▲) for Grande-Rivière anchor station (curves have been vertically offset so as not to overlap). Straight dashed lines show the scaling range

for *in vivo* fluorescence at Grande-Rivière. The mean fractal dimensions of temperature, salinity and *in vivo* fluorescence were respectively 1.54 ( $\pm 0.02$  SE), 1.69 ( $\pm 0.03$  SE) and 1.48 ( $\pm 0.02$  SE) at Caplan, and 1.5 ( $\pm 0.03$  SE), 1.57 ( $\pm 0.02$  SE) and 1.59 ( $\pm 0.01$  SE) at Grande-Rivière. The mean empirical estimates of the

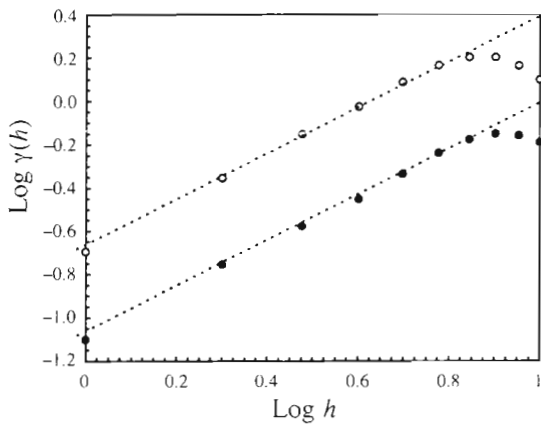


Fig. 9. Double logarithmic semivariograms of temperature at 4 m depth for Caplan anchor station before (○) and after (●) destratification by wind

fractal dimensions  $D_F$  of temperature, salinity and *in vivo* fluorescence exhibited different patterns of variation within stations and between stations. Thus, we showed that there were significant differences between salinity, temperature and *in vivo* fluorescence fractal dimensions for either station (Kruskal-Wallis test,  $p < 0.05$ ). However, at Caplan mean fractal dimensions  $D_F$  of temperature, salinity and *in vivo* fluorescence were significantly different from each other (Jonckheere test,  $p < 0.05$ ; Siegel & Castellan 1988), whereas at Grande-Rivière, mean fractal dimensions of salinity and *in vivo* fluorescence were not significantly different but were both significantly different from that of temperature (Jonckheere test,  $p > 0.05$  and  $p < 0.05$ , respectively). On the other hand, mean fractal dimensions of salinity and *in vivo* fluorescence were significantly different between the 2 stations (Wilcoxon-Mann-Whitney  $U$ -test,  $p < 0.05$ ), whereas there was no significant difference between mean fractal dimensions of temperature (Wilcoxon-Mann-Whitney  $U$ -test,  $p > 0.05$ ). Fractal dimension  $D_F$  plotted as a function of depth (Fig. 10) leads to further conclu-

sions. At Caplan (Fig. 10a),  $D_F$  of temperature, salinity and *in vivo* fluorescence exhibited similar patterns of variation, with a maximum value between 12 and 14 m depth, suggesting the influence of internal waves. In contrast, at Grande-Rivière the situation was quite different (Fig. 10b): fractal dimensions of temperature and *in vivo* fluorescence exhibit respectively maximum and minimum values around 10 m depth, while  $D_F$  of salinity exhibited a tendency to decrease from the sub-surface to bottom.

### DISCUSSION

The empirical estimates of the mean fractal dimensions  $D_F$  showed that the mean  $D_F$  of temperature is smaller than that of *in vivo* fluorescence and salinity at Caplan. This can be related with the processes likely to influence the variability of both temperature (T) and salinity (S). The T-S diagram (Fig. 11a) suggests an almost linear mixing of relatively warm ( $T > 14^\circ\text{C}$ ) and weakly saline ( $27.5 < S < 29.5\text{‰}$ ) waters (A), with colder ( $T < 14^\circ\text{C}$ ) more saline ( $S > 29.5\text{‰}$ ) waters (B), characteristic of the eastern part and to the mouth of

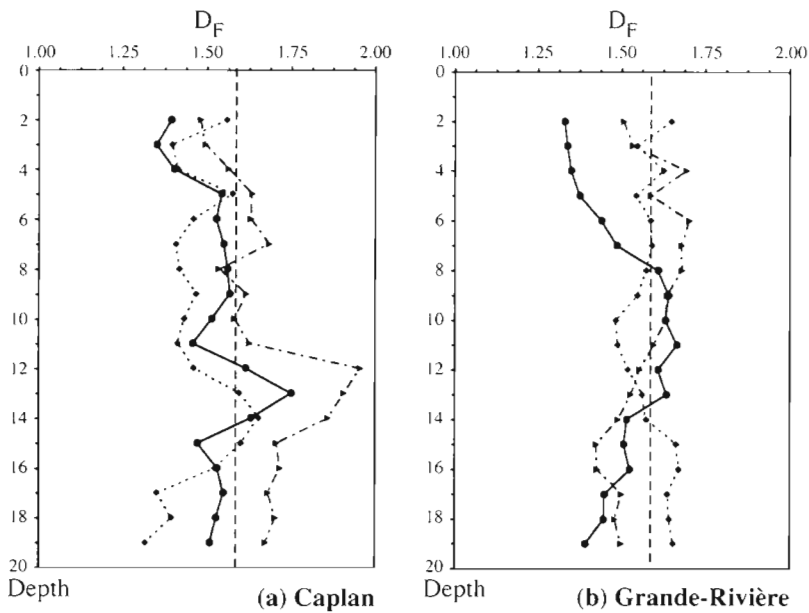


Fig. 10. Fractal dimensions ( $D_F$ ) of *in vivo* fluorescence (◆), temperature (●) and salinity (▲) in relation to depth for (a) Caplan and (b) Grande-Rivière anchor stations. Straight broken lines correspond to the theoretical case  $D_F = -5/3$

the bay, respectively (Legendre 1987). This distribution of water masses is associated with the cyclonic circulation of the Baie des Chaleurs observed during the sampling experiment (Le Quéré 1992) and has already been suggested to potentially modify the water mass properties of the Baie des Chaleurs by vertical mixing (Legendre & Watt 1970, Legendre 1987). Moreover, temperature fluctuations are mainly dependent on atmospheric (i.e. seasonal) warming and cooling whereas salinity is mainly influenced by river and precipitation runoffs leading to smaller scales variations. The intermediate value of the fractal dimension of *in vivo* fluorescence might then be regarded as a result of the interactions between these 2 different forcings. At Grande-Rivière the mean fractal dimension of temperature is smaller than those of salinity and *in vivo* fluorescence, which are not significantly different, indicating that variability of biological processes is mainly determined by salinity and is characterised by short-range variations in comparison with temperature. Indeed, the T-S diagram (Fig. 11b) shows the strong influence of weakly saline ( $S < 29.5\text{‰}$ ) waters, different from the water masses typical of the mouth of the bay (B, Fig. 11a) and associated with the rise of a west-southwest heavy swell after the 30th profile (cf. Fig. 3) of the sampling experiment. The properties of these water masses (i.e. in terms of temperature and salinity) are roughly similar to those observed in the upper water masses of the Gulf of St. Lawrence, Canada (Lauzier 1957, Dickie & Trites 1983). The shift in the main current direction associated with the rising swell

can then be suggested as being caused by the strengthening of the influence of the Gaspé current (Bugden 1981) on the northern coast of the Baie des Chaleurs, where it is usually weak, indeed lacking, as previously observed (Le Quéré 1992, Bonardelli et al. 1993). The associated time scales are then small compared with those associated with the seasonal forcing on temperature variability, leading to a perceived higher homogeneity.

The different fractal dimensions observed between stations lead to further conclusions. Mean fractal dimensions of temperature are not significantly different, whereas mean fractal dimensions of salinity and *in vivo* fluorescence are significantly different at Caplan to those at Grande-Rivière. This suggests that the physical forcings (i.e. mainly atmospheric) responsible for the temperature variability are on an equivalent space-

time scale at Caplan and Grande-Rivière. On the other hand, salinity appears to be associated with more homogeneous space-time patterns at Caplan than at

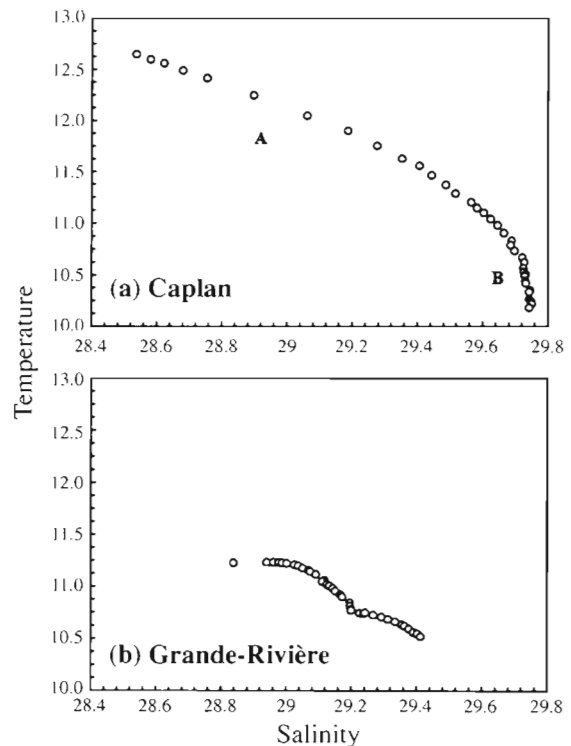


Fig. 11. Temperature-salinity diagrams for (a) Caplan (for explanation of A and B see 'Discussion') and (b) Grande-Rivière anchor stations

Grande-Rivière (i.e.  $D_F$  was greater at Caplan, showing the predominance of short-range processes at Caplan). This last observation agrees with our previous observations concerning the different forcing processes at Caplan and Grande-Rivière. In contrast, *in vivo* fluorescence shows a more heterogeneous structuration at Caplan than at Grande-Rivière (i.e.  $D_F$  greater at Grande-Rivière), indicating the prevalence of short-range variability and thus of biological processes when the hydrodynamical forcings are less developed (cf. Figs. 2 to 5).

Comparison of the estimated mean fractal dimensions of temperature, salinity and *in vivo* fluorescence with those of other environmental data shows that the variations of these variables are always more homogeneous than those of landform (Mandelbrot 1977), seismicity frequency (Khatti 1995), river discharge, geological sediment and climate data (Mandelbrot & Wallis 1969), and more homogeneous than the variability perceived in soil properties (Burrough 1981, 1983a), spatial distribution of plant communities (Palmer 1988) and spatial distribution of marine birds and their zooplanktonic preys (Russel et al. 1992). We have no clear phenomenological explanation for these differences, though empirical  $D_F$  might be directly linked to the nature of the processes generating the observed patterns. Indeed, geological fluctuations associated with earthquake occurrence are associated with large-scale processes (in time or space; e.g. periods of about 100 yr; see e.g. Khattri 1995) and lead to low fractal dimensions corresponding to long-range trends and thus to a great heterogeneity. In contrast, fluctuating data associated with smaller-scale processes, such as turbulent motion, widely recognised as a controlling factor of plankton distribution (Legendre & Demers 1984, Mackas et al. 1985), are expected to lead to higher fractal dimensions (Burrough 1981, 1983a). Our empirical  $D_F$  can also be compared to the fractal dimension  $D_\beta$  estimated from the theoretical spectral exponent  $\beta$  ( $\beta = 5/3$ ) characterising isotropic and homogeneous turbulent processes (Kolmogorov 1941, Obukhov 1941).  $D_\beta$  is estimated as  $D_\beta = 2 - (\beta - 1)/2$  (Feder 1988, Schroeder 1991). From a statistical viewpoint, most  $D_F$  are significantly different from  $D_\beta$  (modified *t*-test; Scherrer 1984). Moreover, as previously suggested,  $D_F$  values reflect the balance of short- and long-range variations, and therefore the differences observed between  $D_F$  and  $D_\beta$  are associated with the theoretical spectral exponent  $\beta$ , as the differences observed in the empirical estimations of  $\beta$  might be related to the different space-time scales of the related external physical forcings (Platt 1972, Denman & Platt 1975, 1976, Platt & Denman 1975, Powell et al. 1975, Fasham & Pugh 1976, Denman et al. 1977, Horwood 1978, Lekan & Wilson 1978, Demers et al. 1979, Wiegand & Pond 1979, Seuront et al. 1996a, b, Seuront 1997).

At Caplan, no differences could be observed in the fractal dimensions of the data from the first and second day despite the increase in wind speed. Generally speaking, mixing processes in the ocean are responsible for the transfer of kinetic energy from the largest to the smallest scales, spanning several orders of magnitude from the basin scales down to the viscous scales (i.e. the Kolmogorov length scale,  $\lambda_k$ ) at which turbulent energy is dissipated as heat by molecular viscosity (Denman & Gargett 1995). The range of spatial scales over which turbulence, or at least mixing, occurs is intrinsically linked to the dissipation rate of turbulent kinetic energy ( $\epsilon$ ) by the way of the Kolmogorov length and time scales  $\lambda_k$  and  $\tau_k$  [ $\lambda_k = (v^3/\epsilon)^{1/4}$  and  $\tau_k = (v/\epsilon)^{1/2}$ , where  $v$  is the kinematic viscosity) and thus to the hydrodynamic conditions. The dissipation rate of wind turbulent kinetic energy  $\epsilon$  ( $\text{m}^2 \text{s}^{-3}$ ) was estimated as  $\epsilon = (5.82 \times 10^{-9})W^3/z$ , where  $W$  is the wind speed ( $\text{m s}^{-1}$ ) and  $Z$  the depth (m) (MacKenzie & Leggett 1993). This dissipation rate, averaged over the water column for the 2 periods (i.e. before and after the increase in the wind speed), increased from  $7.18 \times 10^{-9} \text{ m}^2 \text{ s}^{-3}$  to  $3.01 \times 10^{-7} \text{ m}^2 \text{ s}^{-3}$ , leading to a decrease in the Kolmogorov length and time scales  $\lambda_k$  and  $\tau_k$  (from 3.43 to 1.35 mm and from 11.78 to 1.82 s, respectively) and thus to an increase in the range of time and space scales affected by turbulent motions. However, this increase in the range of turbulent space-time scales is far from being perceptible from our hourly sampling interval which can thus be proposed to explain the non significant differences between fractal dimensions before and after the destratification of the water column by wind (cf. Fig. 9) and thus does not allow any inferences about the effects of varying hydrodynamic conditions on the structure—in terms of homogeneity or heterogeneity, and thus in terms of short- or long-range variability—of this pelagic environment. Moreover, the structure of phytoplankton biomass appears to be independent of the concentration since a decrease of 40% of the total biomass between the first and the second part of the cruise (Raby et al. 1994) was not associated with a change in the estimated fractal dimension or the characteristic scale-breaking observed in the semi-variograms. Furthermore, as the phytoplankton assemblage was very similar over the sampling period (Mingelbier 1995), we cannot test any potential specific effects on fluorescence fractal dimensions.

On the other hand, it is worth noting that the vertical distribution of the mean  $D_F$  of temperature, salinity and *in vivo* fluorescence at Caplan (Fig. 10a) can be related to the time-averaged vertical distribution of the Richardson number,  $Ri$  (Fig. 12a). The minimum and maximum values of  $D_F$  can be associated respectively with the least stable (i.e. low  $Ri$ , surface layers and near the bottom) and stable (i.e. high  $Ri$ , mid-depth)

water masses. Thus, in surface layers and near the bottom, where mixing processes are more developed, the low dynamic stability leads to low fractal dimensions showing—at the time-space scales of the study—the predominance patterns irregularly distributed in space and time and thus, characterised by long-range variations. On the other hand, at mid-depth, the greater dynamic stability tends to damp out any kind of fluctuations, leading to less structured patterns with close scales of variation, characterised by higher fractal dimensions and suggesting a potential aliasing of internal waves. The situation is quite different at Grande-Rivière (Fig. 10b), where the maximum value of the mean  $Ri$  (Fig. 12b) can be related to the maximum and minimum values of the fractal dimensions of temperature and *in vivo* fluorescence, respectively. This last observation shows that in weak hydrodynamic conditions *in vivo* fluorescence exhibits a very specific behaviour, far from physical control, showing that the biological activity and its associated variability are more developed in stable conditions (i.e. high  $Ri$ ). In the case of salinity, we have no clear explanation to propose for the decreasing tendencies of the mean fractal dimension which can, however, be related to the interactions between the characteristic water masses of the mouth of the bay and the water masses advected by the west-southwest drift induced by the swell. Consequently, the differences observed between our low and high empirical  $D_F$  can be explained in terms of different range of scales perceived in pattern variability and thus in the complexity of the pattern structure.

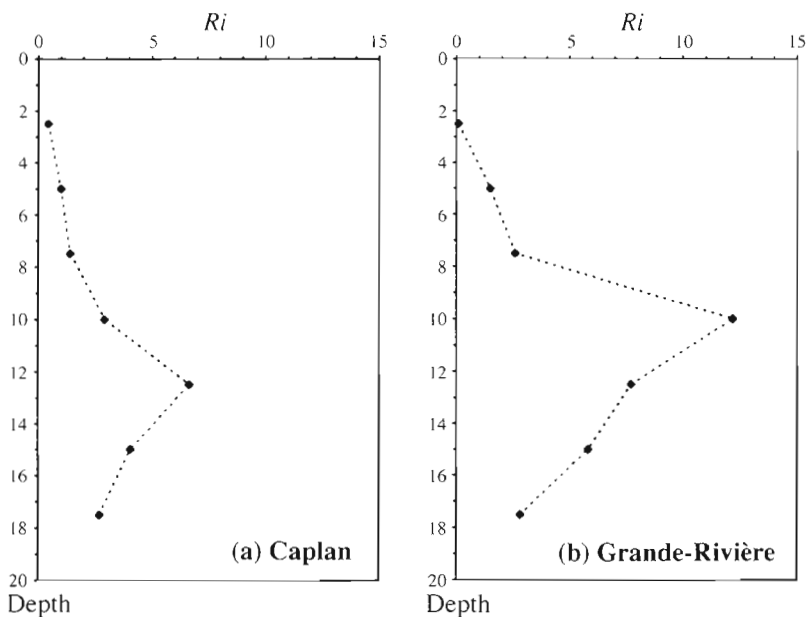


Fig. 12. Time-averaged Richardson number ( $Ri$ ) in relation to depth for (a) Caplan and (b) Grande-Rivière anchor stations

Beyond the numerical values of fractal dimensions, semivariogram analysis can also provide information about the scaling behaviour of a given process. Thus, the fractal dimension is not necessarily a constant over varying sampling intervals (Palmer 1988). We cannot test the scale invariance of temporal patterns of temperature, salinity and *in vivo* fluorescence in that way because of the small number of data values available in the analysis and because the semivariance does not always increase monotonically with increasing lag (Fig. 7), but appears to increase in a series of steps (Figs. 7 & 8). In the case of ideal fractals, like Brownian fractal functions (Burrough 1983a, b), the semivariogram shows clear range and sill (e.g. see Phillips 1985 for further details), leading to the assertion that the data show at least local second-order stationarity (Journel & Huijbregts 1978). Increasing the size of the inter-sample distance, however, frequently leads to observation of increased semivariance (Burrough 1983a) implying that new scales of variation have been encountered. This stepwise behaviour (i.e. changes in fractal dimension when shifting between scales) implies that in place of true self-similarity, temperature, salinity and *in vivo* fluorescence show only partial self-similarity over limited range of scales separated by transition zones (Mandelbrot 1977, 1983), where the environmental properties or constraints acting upon organisms are probably changing rapidly (Frontier 1987; also e.g. the landscape patterns analysed by Krummel et al. 1987 and Palmer 1988). In the Baie des Chaleurs (i.e. at Caplan and Grande-Rivière), the departures from true self-similarity seem to be associated

with the progressive change in the eulerian residual circulation with depth (cf. Figs. 2 & 3). Indeed, the change of direction of the eulerian residual circulation can be suggested as a possible source of scale breaking between scale dependence and scale independence, in so far as the loss of self-similarity of semivariograms seems to be associated with the depth, showing a reversal in the direction of the residual circulation of water masses (Figs. 2 & 3). These factors, their combinations and/or the interactions with water masses coming from river discharge or outside the bay can be proposed as possible sources of variability and thus could be responsible not only for the different time scales of temporal dependence of variogram analysis but also for the absence of scale-invariant structuration after the scale breaking. These departures

from true self-similarity, rather than the precise numerical values of the fractal dimension, may be of most interest to ecologists, because such departures indicate variation in the sources of biological patterns (Burrough 1983a, Bradbury et al. 1984, Russel et al. 1992). As an example, the critical range represented by the well-known 'Platt-knee' corresponds to the transition zone (at a scale between 0.2 and 20 km; Platt & Denman 1975, Denman & Platt 1976, Denman et al. 1977) between scales dominated by physical processes and larger scales dominated by the combination of biological activities, such as growth, sinking, or community interactions. However, unlike the previous case, our results do not show any characteristic scales which can be obviously related to a well-known physical or biological transition zone.

To date, most studies using fractal approaches have focused on phenomena which are temporally invariant over the scale of the study (e.g. vegetation patterns, Palmer 1988; coral reefs structure, Bradbury & Reichelt 1983, Bradbury et al. 1984; or geological formations, Burrough 1983a) and we are not aware of any reports of a temporal fractal approach. However, our sampling experiments have been conducted at anchor stations (i.e. an eulerian point of view), so that temporal and spatial components of variation are inextricably confounded in our data. This confounding of space and time has already been pointed out by Russel et al. (1992) in a study of the 'spatial' distributions of marine birds and their food and might be suggested as a possible source of bias in the estimation of fractal dimensions. Nonetheless, the estimated fraction dimensions are consistent with the global physical structure of both stations and can thus be regarded as a useful index of the complexity perceived in time series of temperature, salinity and *in vivo* fluorescence.

These results, suggesting relationships exist between the vertical structure of the water column (i.e. dynamic stability and residual circulation), fractal dimensions and the characteristic scale breaking between temporal dependence and independence thus lead us to consider a physical control of temperature, salinity and *in vivo* fluorescence variability at Caplan associated with high hydrodynamic conditions and a slightly more complex situation at Grande-Rivière, where, probably because of the weak hydrodynamism and the peculiar pattern of water masses circulation, temperature, salinity and *in vivo* fluorescence exhibit more specific patterns of variations. However, it can also be suggested that the differences observed between fractal dimensions may be caused by processes exhibiting very specific intermittent behaviours. Indeed, previous studies conducted on zooplankton data (Pascual et al. 1995), temperature and *in vivo* fluorescence (Seuront et al. 1996a, b) have shown that the best tool to describe intermittent fields is

provided by multifractal theory. Multifractal analysis, inadequate in the present study because of the small number of data available, can be regarded as a statistical generalisation of fractal theory (Mandelbrot 1977, 1983) leading to the consideration of multifractal fields as a hierarchy of sets each with its own fractal dimension. Thus multifractal fields are described by scaling relations that require a family of different exponents, rather than the single exponent of 'traditional' fractal patterns, which then characterise variability in a very limited way. Furthermore, despite the apparent complexity induced by a multifractal framework, using the universal multifractal formalism (Schertzer & Lovejoy 1987, 1989)—recently successfully applied to oceanic fields (Seuront et al. 1996a, b, Seuront 1997)—the distribution of a scalar field can be wholly described with only 3 indices, which summarise the whole statistical behaviour from larger to smaller scales.

Nevertheless, fractals provide a workable middle ground between the excessive geometric order of Euclid and the geometric chaos of roughness and fragmentation (Mandelbrot 1989), and appear to be particularly well adapted to the study of multiscale environments such as pelagic ecosystems. However, even though the results of this fractal analysis should have probably been more illustrative by considering a finer grain and a greater extent, which are often regarded as some of the main aspects of the scales of a study (Legendre & Fortin 1989, Wiens 1989, Jarvis 1995), they are consistent with more classical techniques concerning the time-space physical structure of the studied environments, and thus appear to be quite satisfactory. Furthermore, the value of geostatistical analysis is that different and complex dynamics can be described in a common format that allows direct comparisons to be made among systems. One should be aware, however, that the generic name 'fractal dimension' deals with different concepts of dimensions: topological dimension, Hausdorff dimension, self-similarity dimension, box-counting dimensions and information dimension among others. They are all related, sometimes they are the same and sometimes different, and that can be confusing even for a research mathematician (Peitgen et al. 1992). Practically, for ecologists, this means that at present it is only possible to compare different estimates of fractal dimension when the same calculation technique is used. There is, therefore, a need to calibrate different methods of calculating fractal dimensions and until this is done, comparisons of  $D_F$  values of similar phenomena reported in the literature, obtained with different techniques, are of limited value.

*Acknowledgements.* We greatly acknowledge C. Luczak and F. Lizon for stimulating and constructive discussions on the subject. We are also thankful to V. Gentilhomme for her com-

ments on the manuscript and to D. Schertzer, F. Schmitt and 4 anonymous referees for their remarks and suggestions which greatly improved the manuscript.

## LITERATURE CITED

- Berry MV, Lewis ZV (1980) On the Weierstrass-Mandelbrot fractal function. *Proc R Soc Lond A* 370:459–484
- Bivand R (1980) A Monte Carlo study of correlation coefficient estimation with spatially autocorrelated observations. *Quaest Geogr* 6:5–10
- Bonardelli JC, Himmelman JH, Drinkwater K (1993) Current variability and upwelling along the North shore of Baie des Chaleurs. *Atmos-Ocean* 31:541–565
- Bradbury RH, Reichelt RE (1983) Fractal dimension of a coral reef at ecological scales. *Mar Ecol Prog Ser* 10:169–171
- Bradbury RH, Reichelt RE, Green DG (1984) Fractals in ecology: methods and interpretation. *Mar Ecol Prog Ser* 14:295–296
- Bugden GL (1981) Salt and heat budgets for the Gulf of St-Lawrence. *Can J Fish Aquat Sci* 38:1153–1167
- Bundy MH, Gross TF, Coughlin DJ, Strickler JR (1993) Quantifying copepod searching efficiency using swimming patterns and perceptive ability. *Bull Mar Sci* 53:15–28
- Burrough PA (1981) Fractal dimensions of landscape and other environmental data. *Nature* 294:240–242
- Burrough PA (1983a) Multiscale sources of spatial variation in soil. I. The application of fractal concepts to nested levels of soil variation. *J Soil Sci* 34:577–597
- Burrough PA (1983b) Multiscale sources of spatial variation in soil. II. A non-Brownian fractal model and its application to soil survey. *J Soil Sci* 34:599–620
- Demers S, Lafleur PE, Legendre L, Trump CL (1979) Short-term covariability of chlorophyll and temperature in the St. Lawrence Estuary. *J Fish Res Bd Can* 36:568–573
- Denman KL, Gargett AE (1995) Biological-physical interactions in the upper ocean: the role of vertical and small scale transport processes. *Annu Rev Fluid Mech* 27:225–255
- Denman KL, Okubo A, Platt T (1977) The chlorophyll fluctuation spectrum in the sea. *Limnol Oceanogr* 22:1033–1038
- Denman KL, Platt T (1975) Coherences in the horizontal distributions of phytoplankton and temperature in the upper ocean. *Mém Soc R Sci Liège Collect* 6:19–30
- Denman KL, Platt T (1976) The variance spectrum of phytoplankton in a turbulent ocean. *J Mar Res* 34:593–601
- Denman KL, Powell TM (1984) Effects of physical processes on planktonic ecosystems in the coastal ocean. *Oceanogr Mar Biol Annu Rev* 22:125–168
- Dickie LM, Trites RW (1983) The Gulf of St-Lawrence. In: Ketchum BH (ed) *Estuaries and enclosed seas*. Elsevier, Amsterdam, p 403–425
- Downing JA (1991) Biological heterogeneity in aquatic ecosystems. In: Kolasa J, Pickett STA (eds) *Ecological heterogeneity*. Springer Verlag, New York, p 160–180
- Downing JA, Pérusse M, Frenette Y (1987) Effect of inter-replicate variance on zooplankton sampling design and data analysis. *Limnol Oceanogr* 32:673–680
- Dutilleul P, Legendre P (1993) Spatial heterogeneity against heteroscedasticity: an ecological paradigm versus a statistical concept. *Oikos* 66:152–171
- Erlandson J, Kostylev V (1995) Trail following, speed and fractal dimension of movement in a marine prosobranch, *Littorina littorea*, during a mating and a non-mating season. *Mar Biol* 122:87–94
- Falkowski PG, Kiefer DA (1985) Chlorophyll a fluorescence in phytoplankton: relationship to photosynthesis and biomass. *J Plankton Res* 7:715–731
- Fasham MJR, Pugh PR (1976) Observations on the horizontal coherence of chlorophyll *a* and temperature. *Deep Sea Res* 23:527–538
- Feder J (1988) *Fractals*. Plenum, New York
- Frontier S (1972) Calcul de l'erreur sur un comptage de zooplancton. *J Exp Mar Biol Ecol* 8:121–132
- Frontier S (1985) Diversity and structure in aquatic ecosystems. *Oceanogr Mar Biol Annu Rev* 23:253–312
- Frontier S (1987) Applications of fractal theory to ecology. In: Legendre P, Legendre L (eds) *Developments in numerical ecology*. Springer Verlag, Berlin, p 335–378
- Frontier S (1994) Species diversity as a fractal property of biomass. In: Nowak MM (ed) *Fractals in the natural and applied sciences (A-41)*. Elsevier, Amsterdam, p 119–127
- Gee JM, Warwick RM (1994a) Body-size distribution in a marine metazoan community and the fractal dimensions of macroalgae. *J Exp Mar Biol Ecol* 178:247–259
- Gee JM, Warwick RM (1994b) Metazoan community structure in relation to the fractal dimensions of marine macroalgae. *Mar Ecol Prog Ser* 103:141–150
- Grey-Smith P (1979) Pattern in vegetation. *J Ecol* 67:755–779
- Hairy LR, McGowan JA, Wiebe PH (1978) Patterns and processes in the time-space scales of plankton distributions. In: Steele JH (ed) *Spatial pattern in plankton communities*. Plenum, New York, p 277–327
- He F, Legendre P, Bellehumeur C (1994) Diversity pattern and spatial scale: a study of a tropical rain forest of Malaysia. *Environ Ecol Stat* 1:265–286
- Horwood JW (1978) Observations on spatial heterogeneity of surface chlorophyll in one and two dimensions. *J Mar Biol Assoc UK* 58:487–502
- Hurlbert SH (1990) Spatial distribution of the montane unicorn. *Oikos* 58:257–271
- Ibanez F, Fromentin JM, Castel J (1993) Application de la méthode des sommes cumulées à l'analyse des séries chronologiques en océanographie. *C R Acad Sci Paris* 316:745–748
- Jarvis PG (1995) Scaling processes and problems. *Plant Cell Environ* 18:1079–1089
- Journel AG, Huijbregts CJ (1978) *Mining geostatistics*. Academic Press, London
- Kaandorp JA (1991) Modelling growth forms of the sponge *Haliclona oculata* (Porifera, Demospongiae) using fractal techniques. *Mar Biol* 110:203–215
- Kaandorp JA, Dekhuijver MJ (1992) Verification of fractal growth models of the sponge *Haliclona oculata* (Porifera) with transplantation experiments. *Mar Biol* 113:133–143
- Kendall M (1976) *Time-series*, 2nd edn. Charles Griffin and Co Ltd, London
- Kendall M, Stuart A (1966) *The advanced theory of statistics*. Hafner, New York
- Khattri KN (1995) Fractal description of seismicity of India and inferences regarding earthquake hazard. *Curr Sci* 69:361–366
- Kolasa J, Rollo DC (1991) The heterogeneity of heterogeneity: a glossary. In: Kolasa J, Pickett STA (eds) *Ecological heterogeneity*. Springer Verlag, New York, p 1–23
- Kolmogorov AN (1941) The local structure of turbulence in incompressible viscous fluid with very large Reynolds numbers. *Dokl Akad Nauk SSSR* 30:299–303
- Krummel JR, Gardner RH, Sugihara G, O'Neill RV, Coleman PR (1987) Landscape patterns in a disturbed environment. *Oikos* 48:321–324
- Lagadeuc Y, Boulé M, Dodson JJ (1997) Effect of vertical mixing on the vertical distribution of copepods in coastal

- waters. *J Plankton Res* 19:1183–1204
- Lauzier LM (1957) Variations of temperature and salinity in shallow waters of the southwestern Gulf of St-Lawrence. *Bull Fish Res Bd Can* 111:251–268
- Legendre L (1987) Multidimensional contingency table analysis as a tool for biological oceanography. *Biol Oceanogr* 5: 13–28
- Legendre L, Demers S (1984) Towards dynamic biological oceanography and limnology. *Can J Fish Aquat Sci* 41: 2–19
- Legendre L, Fortin MJ (1989) Spatial pattern and ecological analysis. *Vegetatio* 80:1055–1067
- Legendre L, Legendre P (1984) *Ecologie numérique*, Vol 2, 2nd edn. Masson, Paris
- Legendre L, Watt WD (1970) The distribution of primary production relative to a cyclonic gyre in Baie des Chaleurs. *Mar Biol* 7:167–170
- Lekan JF, Wilson RE (1978) Spatial variability of phytoplankton biomass in the surface waters of Long Island. *Estuar Coast Mar Sci* 6:230–251
- Le Quéré C (1992) Physical oceanography of the Baie des Chaleurs, Gulf of St. Lawrence. MSc thesis, McGill University, Montréal
- Li X, Logan BE (1995) Size distribution and fractal properties of particles during a simulated bloom in a mesocosm. *Deep Sea Res I* 42:125–138
- Lizon F, Lagadeuc Y, Brunet C, Aelbrecht D, Bentley D (1995) Primary production and photoadaptation of phytoplankton in relation with tidal mixing in coastal waters. *J Plankton Res* 17:1039–1055
- Logan BE, Kilps JR (1995) Fractal dimensions of aggregates formed in different fluid mechanical environments. *Wat Res* 29:443–453
- Longuet-Higgins MS (1994) A fractal approach of breaking waves. *J Phys Oceanogr* 24:1834–1838
- Lovejoy S (1982) Area-perimeter relation for rain and cloud areas. *Science* 216:185–187
- Mackas DL, Boyd CM (1979) Spectral analysis of zooplankton spatial heterogeneity. *Science* 204:62–64
- Mackas DL, Denman KL, Abbot MR (1985) Plankton patchiness: biology in the physical vernacular. *Bull Mar Sci* 37:652–674
- MacKenzie BR, Leggett WC (1993) Wind-based models for estimating the dissipation rates of turbulence energy in aquatic environments: empirical comparisons. *Mar Ecol Prog Ser* 94:207–216
- Mandelbrot B (1977) *Fractals. Form, chance and dimension*. Freeman, London
- Mandelbrot B (1983) *The fractal geometry of nature*. Freeman, New York
- Mandelbrot B (1989) Fractal geometry: what is it and what does it do? In: Fleischmann M, Tildesley DJ, Ball RC (eds) *Fractals in the natural sciences*. Princeton University Press, Princeton, NJ, p 3–16
- Mandelbrot B, Wallis JR (1969) Some long-run properties of geophysical records. *Wat Resour Res* 5:321–340
- Mann KH, Lazier JRN (1991) *Dynamics of marine ecosystems. Biological-physical interactions in the ocean*. Blackwell Scientific Publications, Boston
- Matheron G (1971) La théorie des variables régionalisées et ses applications. *Cah CMM Fontainebleau* 5:1–212
- Milne BT (1988) Measuring the fractal geometry of landscapes. *Appl Math Comput* 27:67–79
- Mingelbier M (1995) Contrôle différentiel de la taille du phytoplancton marin dans les eaux côtières tempérées (Baie des Chaleurs, Golfe du St Laurent). PhD thesis, Université Laval
- Naeem S, Colwell RK (1991) Ecological consequences of heterogeneity of consumable resources. In: Kolasa J, Pickett STA (eds) *Ecological heterogeneity*. Springer Verlag, New York, p 224–255
- Obukhov AM (1941) Spectral energy distribution in a turbulent flow. *Dokl Akad Nauk SSSR* 32:22–24
- Olsson J, Niemczynowicz J, Berndtsson R, Larson L (1992) An analysis of the rainfall time structure by box counting—some practical implications. *J Hydrol* 137:261–277
- Palmer MW (1988) Fractal geometry: a tool for describing spatial patterns of plant communities. *Vegetatio* 75:91–102
- Pascual M, Ascoti FA, Caswell H (1995) Intermittency in the plankton: a multifractal analysis of zooplankton biomass variability. *J Plankton Res* 17:1209–1232
- Peitgen HO, Jügens H, Saupe D (1992) *Chaos and fractal: new frontiers of science*. Springer-Verlag, New York
- Pennycuik CJ, Kline NC (1986) Units of measurement for fractal extent, applied to the coastal distribution of bald eagle nests in the Aleutian Islands, Alaska. *Oecologia* 68: 254–258
- Phillips JD (1985) Measuring complexity of environmental gradients. *Vegetatio* 64:95–102
- Platt T (1972) Local phytoplankton abundance and turbulence. *Deep Sea Res* 19:183–187
- Platt T, Denman KL (1975) Spectral analysis in ecology. *Annu Rev Ecol Syst* 6:189–210
- Platt T, Sathyendranath S (1988) Oceanic primary production: estimation by remote sensing at local and regional scales. *Science* 241:1613–1620
- Pond S, Pickard GL (1983) *Introductory dynamical oceanography*, 2nd edn. Pergamon Press, Oxford
- Powell TM, Richerson PJ, Dillon TM, Agee BA, Dozier BJ, Godden DA, Myrup LO (1975) Spatial scales of current speed and phytoplankton biomass fluctuations in Lake Tahoe. *Science* 189:1088–1090
- Raby D, Lagadeuc Y, Dodson JJ, Mingelbier M (1994) Relationship between feeding and vertical distribution of bivalve larvae and mixed waters. *Mar Ecol Prog Ser* 130: 275–284
- Risser PG, Karr JR, Forman RTT (1984) *Landscape ecology: directions and approaches*. Nat Hist Surv Spec Pub No. 2
- Russel RW, Hunt GL, Coyle KO, Cooney RT (1992) Foraging in a fractal environment: spatial patterns in a marine predator-prey system. *Landscape Ecol* 7:195–209
- Scherrer B (1984) Biostatistiques. Gaëtan Morin, Boucherville
- Schertzer D, Lovejoy S (1987) Physically based rain and cloud modeling by anisotropic multiplicative turbulent cascades. *J Geophys Res* 92:9693–9714
- Schertzer D, Lovejoy S (1989) Nonlinear variability in geophysics: multifractal analysis and simulation. In: Pietronero L (ed) *Fractals: physical origin and consequences*. Plenum, New York, p 49–79
- Schroeder M (1991) *Fractals, chaos, power laws. Minutes from an infinite paradise*. Freeman, New York
- Seuront L (1997) Distribution inhomogène multi-échelle de la biomasse phytoplanctonique en milieu turbulent. *J Rech Océanogr* 22:9–16
- Seuront L, Schmitt F, Lagadeuc Y, Schertzer D, Lovejoy S, Frontier S (1996a) Multifractal analysis of phytoplankton biomass and temperature in the ocean. *Geophys Res Lett* 23:3591–3594
- Seuront L, Schmitt F, Schertzer D, Lagadeuc Y, Lovejoy S (1996b) Multifractal intermittency of Eulerian and Lagrangian turbulence of ocean temperature and plankton fields. *Nonlin Proc Geophys* 3:236–246
- Shachak M, Brand S (1991) Relations among spatiotemporal heterogeneity, population abundance, and variability in a

- desert. In: Kolasa J, Pickett STA (eds) Ecological heterogeneity. Springer Verlag, New York, p 202–223
- Siegel S, Castellan NJ (1988) Nonparametric statistics. McGraw-Hill, New York
- Simpson, JH, Edelsten DJ, Edwards A, Morris NCG, Tett PB (1979) The Islay front: physical structure and phytoplankton distribution. *Estuar Coast Mar Sci* 9:713–726
- Sokal RR, Rohlf FJ (1995) Biometry. The principles and practice of statistics in biological research. Freeman, San Francisco
- Steele JH (1974) The structure of marine ecosystems. Harvard University Press, Boston
- Steele JH (1978) Some comments on plankton patches. In: Steele JH (ed) Spatial patterns in plankton communities. Plenum Press, New York, p 1–20
- Steele JH (1985) A comparison of terrestrial and marine systems. *Nature* 313:355–358
- Steele JH (1989) The ocean 'landscape'. *Landscape Ecol* 3: 185–192
- Sugihara G, May RM (1990) Applications of fractals in ecology. *Trends Ecol Evol* 5:79–86
- Taylor LR (1961) Aggregation, variance and the mean. *Nature* 189:732–735
- Urban DL, O'Neill VO, Shugart HH (1987) A hierarchical perspective can help scientists understand spatial patterns. *BioScience* 37:119–127
- Vandevelde T, Legendre L, Therriault JC, Demers S, Bah A (1987) Subsurface chlorophyll maximum and hydrodynamics of the water column. *J Mar Res* 45:377–396
- Wiegand RC, Pond S (1979) Fluctuations of chlorophyll and related physical parameters in British Columbia coastal waters. *J Fish Res Bd Can* 36:113–121
- Wiens JA (1976) Population responses to patchy environments. *Annu Rev Ecol Syst* 7:81–120
- Wiens JA (1989) Spatial scaling in ecology. *Funct Ecol* 3: 385–397
- Wiens JA, Crist TO, With KA, Milne BT (1995) Fractal patterns of insect movement in microlandscape mosaics. *Ecology* 76:663–666
- Woronow A (1981) Morphometric consistency with the Hausdorff-Besicovitch dimension. *Math Geol* 13:201–216
- Zagoruiko NG, Yolkina VN (1982) Inference and data tables with missing values. *Handb Stat* 2:493–500
- Zar JH (1984) Biostatistical analysis. Prentice-Hall International, Englewood Cliffs, NJ

*Editorial responsibility: Otto Kinne (Editor), Oldendorf/Luhe, Germany*

*Submitted: July 8, 1997; Accepted: September 29, 1997  
Proofs received from author(s): November 11, 1997*